Circular dichroism, optical rotation and absolute configuration of 2-cyclohexenone-*cis*-diol type phenol metabolites: redefining the role of substituents and 2-cyclohexenone conformation in electronic circular dichroism spectra†‡

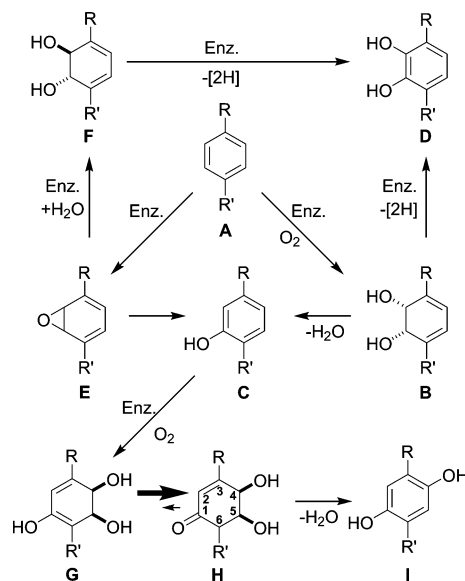**Marcin Kwit,*[a] Jacek Gawronski,[a] Derek R. Boyd,*[b] Narain D. Sharma[b] and Magdalena Kaik[b]**

The absolute configurations of 2-cyclohexenone *cis*-diol metabolites resulting from the biotransformation of the corresponding phenols have been determined by comparison of their experimental and calculated circular dichroism spectra (TDDFT at the PCM/B2LYP/Aug-cc-pVTZ level), optical rotations (calculated at the PCM/B3LYP/Aug-cc-pVTZ level) and by stereochemical correlation. It is found that circular dichroism spectra and optical rotations of 2-cyclohexenone derivatives are strongly dependent on the ring conformation (*M* or *P* sofa S(5) or half-chair), enone non-planarity and the nature and positions of the hydroxy and alkyl substituents. The effect of non-planarity of the enone chromophore, including the distortion of the C═C bond, is determined for the model structures by TDDFT calculations at the PCM/B2LYP/6-311++G(2d,2p) level. Non-planarity of the C═C bond in the enone chromophore is commonly encountered in 2-cyclohexenone derivatives and it is a source of significant rotatory strength contribution to the electronic circular dichroism spectra. It is shown that the two lowest-energy transitions in acrolein and 2-cyclohexenone and its derivatives are $n_{C=O}$–$\pi_{C=O}$* and $\pi_{C=C}$–$\pi_{C=O}$*, as expected, while the shorter-wavelength (below 200 nm) transitions are of more complex nature. In 2-cyclohexenone and its alkyl derivatives it is predominantly a mixture of $\pi_{C=C}$–$\pi_{C=C}$* and $\pi_{C=C}$–σ* transitions, whereas the presence of hydroxy substituent results in a dominant contribution due to the n_{OH}–$\pi_{C=O}$* transition. A generalized model for correlation of the CD spectra of 2-cyclohexenones with their structures is presented.

1. Introduction

Aromatic hydroxylation is among the most common type of enzyme-catalysed reaction of aromatic substrates (**A**) and thus phenols (**C**), catechols (**D**) and hydroquinones (**I**) are generally among the early intermediates formed during the biodegradation of arenes in plants, animals and microorganisms (Scheme 1).[1] The phenolic bioproducts (**C**, **D** and **I**) from aromatic substrates can however be derived from transient or relatively unstable non-aromatic initial metabolites including epoxides (**E**, arene oxides and their oxepine valence tautomers), *cis*-dihydrodiols (**B**) and *trans*-dihydrodiols (**F**) *via* their enzyme-catalysed or spontaneous isomerisation, dehydration or dehydrogenation (Scheme 1). Recent reports on the isolation of relatively stable arene oxides/oxepines (**E**)[2] and *cis*-dihydrodiols (**B**),[3–6] as initial oxidative

[a]Department of Chemistry, A. Mickiewicz University, 60 780 Poznan, Poland. E-mail: Marcin.Kwit@amu.edu.pl; Fax: +48 628291505; Tel: +48 628291367

[b]School of Chemistry and Chemical Engineering, the Queen's University of Belfast, Belfast, BT9 5AG, United Kingdom. E-mail: dr.boyd@qub.ac.uk; Tel: +44 90974687

† Dedicated to Professor Koji Nakanishi on the occasion of his 85th birthday

‡ Electronic supplementary information (ESI) available: Full version of Fig. 5, experimental details, relative energies, structural details for all calculated molecules, calculated ECD data and optical rotations for individual conformers of **1–3** and **4–23**. See DOI: 10.1039/c0ob00422g

Scheme 1 Formation of *cis*-dihydrodiol (**B**), *trans*-dihydrodiol (**F**), cyclohexenone *cis*-diol (**H/G**), arene oxide (**E**) and phenol (**C**, **D**, **I**) metabolites from arenes (**A**).

metabolites of mono- (**A**) or poly-cyclic arenes, is again consistent with the involvement of similar, but less stable, intermediates in the formation of phenols.

A new family of even more stable 2-cyclohexenone *cis*-diols (**H**) derived from phenols (**C**), has recently been isolated in these laboratories.[7] Type **H** bioproducts could be considered as second generation metabolites involving (i) the initial dioxygenase-catalysed *cis*-dihydroxylation of an arene **A** (*e.g.* R = R′ = Me) to yield an unstable *cis*-dihydrodiol **B** (*e.g.* R = R′ = Me), (ii) spontaneous aromatization to form a phenol **C** (*e.g.* R = R′ = Me) and (iii) a second enzymatic *cis*-dihydroxylation to give intermediate **G** (*e.g.* R = R′ = Me) which prefers to exist as the more stable 2-cyclohexenone *cis*-diol tautomer **H** (*e.g.* R = R′ = Me).[7] Most members of the new cyclohexenone *cis*-diol family (**H**) have however been produced *via* biotransformation of the corresponding substituted phenol substrates (**C**). 2-Cyclohexenone *cis*-diols (**H**), obtained using whole cells of a constituent mutant (UV4) of the soil bacterium *Pseudomonas putida* containing toluene dioxygenase (TDO), were in some cases accompanied by catechols (**D**).

In the preliminary report involving a very limited range of cyclohexenone *cis*-diol metabolites **H/G** (R = Me, R′ = H; R = R′ = Me; R = I, R′ = H; R = H, R′ = Me),[7] it was found that they were enantiopure (>98% *ee*) *via* NMR analysis of the corresponding chiral boronate derivatives. Their absolute configurations were mainly determined by a combination of X-ray crystallography **H/G** (R = R′ = Me; R = I, R′ = H) and stereochemical correlation (R = R′ = H; R = CN, R′ = H; R = CO₂Me, R′ = H).

A much wider range of the cyclohexenone *cis*-diol family (**H/G**, >20 members), formed using several dioxygenase types, has now been isolated and structurally characterised.[8] Prior to further studies of the potential of cyclohexenone *cis*-diols **H/G** as synthetic precursors, it was necessary to find a more convenient and generally applicable method for the determination of the absolute configurations of this new class of metabolites. In this context electronic circular dichroism (ECD) spectra and optical rotations (OR), obtained both from experimental measurements and from calculations, have earlier proved to be of considerable value in the assignment of absolute configurations to *cis*-dihydrodiol metabolites. These were obtained from dioxygenase-catalysed *cis*-dihydroxylation of monosubstituted benzenes,[9] disubstituted benzenes[10–12] and from bicyclic aromatics including substituted naphthalene[13] and quinoline[14] ring systems. Based on the calculated ECD and OR values it was possible to provide a rigorous approach to the determination of both preferred conformations and absolute configurations of *cis*-dihydrodiols of type **B**.[9–12]

A major objective of the current study is to determine if a combination of ECD and OR data, obtained by experimental measurement and calculation, can also be applied to new members of the 2-cyclohexenone *cis*-diol family (**H**, R, R′ = H, alkyl)[8] as a reliable method for the assignment of absolute configuration.

A further objective is to determine which structural factors (chromophore nonplanarity, ring conformation, substituents) are primarily responsible for the chiroptical properties (ECD, OR) of 2-cyclohexenone derivatives. The enone chromophore has been a subject of extensive ECD studies in the period of the nineteen sixties to eighties, particularly in relation to *trans*-enone structures present in polycyclic molecules of isoprenoids, including important steroidal hormones (see reviews[15–19]). Empirical rules for planar[20] and twisted[21–24] *trans*-enone chromophores have been postulated on the basis of numerous experimental ECD data, supported by then available theoretical models.[25] A more rigorous

approach to the evaluation of structural factors contributing to the chiroptical properties of *trans*-enones was not available at that time, due to structural complexity of the majority of enones studied and the lack of a practical computational approach to structural and spectroscopic studies of molecules of medium complexity. With simpler 2-cyclohexenone derivatives **H** now available, and DFT computational methods at various levels of accuracy at hand, we felt confident that systematic studies of flexible *trans*-enones would provide a host of information which could be generalized and confronted with the earlier postulated empirical rules. Such an approach has already proven successful for 1,3-cyclohexadiene type metabolites **B**.[9,11,12]

α,β-Unsaturated ketones typically exhibit two absorption bands: one very weak near 330 nm, which is the result of an *n*–π* electronic transition (R-band) and the second around 230 nm which is due to a π–π* electronic transition (K-band). Circular dichroism spectra of α,β-unsaturated ketones exhibit three (sometimes four) Cotton effects between 360 and 185 nm. The weak UV absorption at about 300 nm is responsible for the first long-wavelength Cotton effect of moderate intensity. This band is followed by a π–π* Cotton effect corresponding to the UV band placed within the range 220 and 250 nm. Another Cotton effect that does not have the corresponding UV maximum appears at around 200 nm or at an even higher energy region and usually exhibits high rotatory strength. The origin of this Cotton effect is not clear. Earlier calculations by Liljefors and Allinger suggested that this is another π–π* transition of low intensity in nearly planar enones[26a] and the direction of polarization of this transition has been determined by linear dichroism measurements.[26b]

During the last few decades various chirality rules have been proposed for correlating the Cotton effects of α,β-unsaturated ketones with their stereochemistry. Almost fifty years ago Djerassi,[23] Whalley,[24] and Snatzke,[27] proposed rules for the first two Cotton effects: positive enone helicity was correlated with a negative *n*–π* and a positive π–π* Cotton effect. This rule was thereafter extended by Kirk to *s-cis* and *s-trans* enones unperturbed by polar substituents.[17] Snatzke proposed his own sector rule, a modification of the octant rule that correlates the sign of the *n*–π* Cotton effects with the stereostructure of planar enones.[20,27] The *n*–π* Cotton effects of steroidal enones in oriented (anisotropic) systems were studied by Kuball *et al.*[28] Their studies demonstrated that sector or helicity rules can be applied providing that vibronic progressions originating from various conformers are taken into account.

On the other hand, Burgstahler[29] has shown for the first time the importance of allylic axial substituents that led to a breakdown of the enone helicity rule for the π–π* transition of some *s-cis* steroid enones. The sign of the third electronic transition Cotton effect was correlated with the helicity of the C(axial)–C4–C3=C2 bond system,[15] *P* helicity inducing a positive Cotton effect (for numbering see **H** in Scheme 1).

However, another analysis of the experimental data led to a conclusion that it is the arrangement of the R′–C6–C5–C4–R zig-zag bonds in a 2-cyclohexenone ring, in relation to the enone chromophore, that determines the sign of the short-wavelength Cotton effect.[16]

To the best of our knowledge none of the proposed correlations takes into account a contribution from the twisted C=C bond to the rotatory strength at a given wavelength. Recently Grimme[30]

performed a quantum chemical calculation of the rotatory strength for the electronic transitions of twisted (−10 deg) ethylene. The calculated rotatory strength for the π–π* transition was of the order 75–198 × 10⁻⁴⁰ cgs units, depending on the method used. Since non-planar ethylene generated a high rotatory strength, neglecting such an effect in the case of π–π* electronic transitions of non-planar enone would seem unjustified. Therefore in the later part of our computational studies on variously substituted 2-cyclohexenone molecules we aimed at assessing (i) the rotatory strength generated by a twisted enone and/or a twisted C=C bond in the enone moiety; (ii) the contribution of the saturated C4–C5–C6 bond chain to the rotatory strength of planar and twisted 2-cyclohexenones; (iii) the contributions due to non-polar (methyl) and polar (hydroxy) substituents in various positions of the 2-cyclohexenone skeleton.

2. Results and discussion

2.1 Structures of 2-cyclohexenone *cis*-diols 1–3 from DFT calculations

In order to determine the chiroptical properties of enones **1–3** (Chart 1) with a sufficient level of confidence, structures and conformational equilibria of cyclohexenones **1–3** were calculated at the PCM/MP2/Aug-cc-pVTZ//PCM/B3LYP/6-311++G(2d,2p) level (see Experimental for details). Additional molecules **4–23** were used in this study as model structures to help determine the effect of hydroxy and methyl substituents on the chiroptical properties of 2-cyclohexenones. In the case of compounds **4–23** we used a *P*-helical 2-cyclohexenone as the ring structure, where descriptor *P* indicates the arrangement of the C4–C5–C6 bridge.
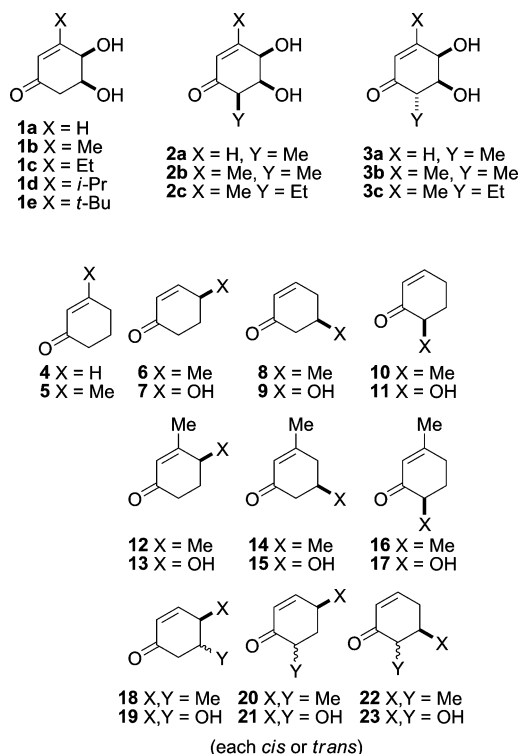
Chart 1

Calculations included both the ring conformers and the substituent rotamers.§ Despite the highly flexible nature of the 2-cyclohexenone skeleton, its principal conformers could be characterized by just a few torsion angles. As shown in Scheme 2 for the assumed 4*R*,5*S* absolute configuration, each ring conformation could be described as either *M* (torsion angles C3–C4–C5–C6 negative, C4–C5–C6–C1 positive, (pseudo)axial C4–OH, (pseudo)equatorial C5–OH or *P* (torsion angle C3–C4–C5–C6 positive, C4–C5–C6–C1 negative, (pseudo)equatorial C4–OH, (pseudo)axial C5–OH). Furthermore, the important enone torsion angle ω (O=C1–C2=C3) can be either very close to 180° (planar enone chromophore) or out of planarity; the same applies to the C1–C2=C3–C4 torsion angle τ.

**Scheme 2** Diastereomeric *P* and *M* conformers of *cis*-ketodiols **1–3** and the definition of torsion angles α, β, ω, τ, φ and φ′.

Calculated structures of individual low-energy conformers of enones **1–3** (for details see Tables A and B in Supplementary Information) are best described as sofa S(5) of either *M* or *P* helicity, with various degrees of distortion from the ideal form, in the direction of a distorted half-chair (HC) conformer. In fact, nearly ideal *M*-S(5) is found in the *M*4 conformer of **1b** and *M*4a conformer of **1c** while a distorted HC structure can be ascribed to *M*1a conformer of **2c** (Fig. 1).

Interestingly, the calculated most stable conformation of the parent 2-cyclohexenone molecule (**4**) was found to be a distorted S(5) structure, with torsion angles ω = 180° and τ close to 0° (see Table B2, Supplementary Information). The energy of the molecule showed little sensitivity to C=C bond twisting (τ 5° to −5°), as long as the torsion angle ω was 180° (Fig. 1(a), Supplementary Information).

The sofa S(5) structure is characterized by a planar enone chromophore, *i.e.* torsion angles ω (O=C1–C2=C3) and τ (C1–C2=C3–C4) ideally are correspondingly 180° and 0°. In a distorted HC conformer the torsion angle ω may be much smaller

§ The use of molecular dynamics for small systems does not provide better results compared to the use of systematical conformational search. In the case of **1e** the number of individual conformers obtained with the use of MD was 5, i.e. less by 2 to that obtained by systematical conformational search.
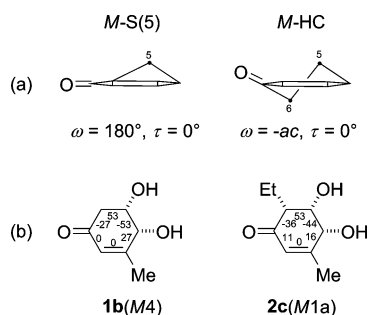
Fig. 1 (a) Structures of sofa S(5) and half-chair HC conformers of the *M* series; (b) ring torsion angles of an ideal sofa conformer of **1b**(*M*4) and a distorted half-chair conformer of **2c**(*M*1a).

(down to ±168°) and the distortion of the C=C bond (angle τ) may reach ±4°. It is of interest to note that the sum of the torsion angles ω and τ is positive for *P* conformers and negative for *M* conformers. Thus the sign of overall distortion of the enone chromophore from planarity conforms to the helicity descriptor *P* or *M*.

As in the case of arene-*cis*-dihydrodiol metabolites[9] the number of available conformers is not limited to *M* and *P* diastereoisomeric structures. Intramolecular hydrogen bond patterns of the hydroxy groups further increase the number of distinct stereoisomeric structures (Scheme 2). Thus, either C4–OH or C5–OH can be a hydrogen bond donor and the orientation of the O–H bond against the vicinal C–H bond can be either *syn* or *anti* (as shown by the corresponding torsion angles α and β). As shown in Scheme 2, up to eight conformers (*M*1–*M*4, *P*1–*P*4) are available but this number can still be greater if one includes the rotamers due to alkyl substituents in the ring, *e.g.* ethyl (**1c**, **2c**, **3c**) and isopropyl (**1d**). Torsion angles α and β fall into the range. ±(147°–179°) for *anti* rotamers and the range is still wider for *syn* rotamers ±(5°– 72°). For the majority of cases the intramolecular hydrogen bond O–H···O is weak (calculated length 2.50 ± 0.15 Å). However, in several conformers of alkylated enones **1c–1e**, **2a–2c** and **3c** (*M*1, *M*2, *P*1, *P*2), this bond is substantially shorter (2.18–2.31 Å). In these conformers the equatorial hydroxy group is a donor to an axial oxygen atom.

The distribution of conformers for each ketodiol **1–3** has been calculated for a free molecule in the gas phase or in a polar medium *i.e.* acetonitrile or methanol. Due to the large number of conformers involved, further analysis was limited to those conformers having contributions over 10% at equilibrium. Fig. 2 shows the calculated distribution of the main conformers in these three different environments.

2-Cyclohexenone-*cis*-diols of 4*R*,5*S* configuration are preferentially of ring *P* helicity in which the allylic hydroxy group is equatorial. Depending on the calculation method used, some conformers were not found as stable structures (for example conformer *P*3 of **1e**). Significant amounts of *M* conformers appear in 3-alkylated enones **1b–1e** and **3a–3c**, since there is a destabilizing interaction between the 3-alkyl and 4-equatorial hydroxy groups. Calculations indicate a high population of *M*4 conformer in the case of the 3-*tert*-butyl derivative **1e**. In the case of compounds **3a–3c**, the equilibrium is additionally driven toward *M* conformers by the equatorial position of the 6-alkyl group. For the same reason, the 6-alkyl substituent in epimeric molecules **2a–2c** additionally
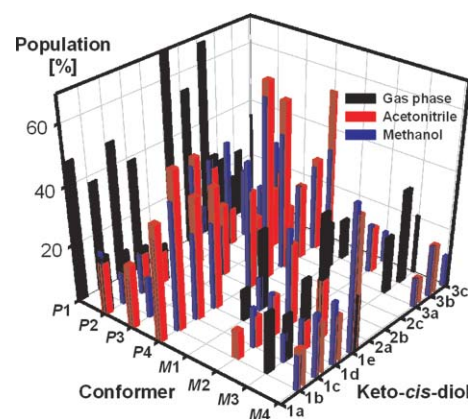

Fig. 2 Populations of main conformers (>10%) of keto-*cis*-diols **1–3** calculated at (PCM)MP2/Aug-cc-pVTZ//(PCM)B3LYP/6-311++G(2d,2p) level for ΔE values. Population of conformers with ethyl and isopropyl substituents is the sum of their rotamers.

stabilizes the *P* conformers so that no significant proportions of conformers *M* can be found by calculation. Another interesting result of calculations is an evident effect of medium polarity on the conformer population. A simulated polar solvent environment (acetonitrile or methanol) brings about the equilibrium shift from *P*1 to *P*3 and *P*4, most evidently seen in the case of enones **1a–1d** and **2a–2c** (Fig. 2). Conformers *P*3 and *P*4, with an equatorial hydroxy group in the allylic position, are apparently better suited for intermolecular hydrogen bonding with the solvent, compared to *P*1 in which the allylic hydroxy group is involved as a donor for intramolecular hydrogen bonding.

2.2 Absolute configurations of 2-cyclohexenone-*cis*-diols 1–3 from circular dichroism and optical rotation data

Earlier studies have shown that the enantiomeric excess values for each of the cyclohexenone *cis*-diols **1a–1e** and **2a–2c** was >98% and that absolute configurations for compounds **1a**, **2a** and **2b** had been unequivocally assigned by stereochemical correlation and X-ray crystallography.[7,8] CD spectra of substituted 2-cyclohexenones **1–3**, of assumed 4*R*,5*S* absolute configuration, were calculated at the PCM/TDDFT/B2LYP/Aug-cc-pVTZ level of theory for each conformer of the relative energy within the 0–2 kcal mol⁻¹ window (see Supplementary Information). After Boltzmann averaging and Gaussian curve fitting[31] the calculated CD spectra of **1–3** were compared with the experimental ones, as shown in Fig. 3 and 4.

The calculated CD curves were wavelength-corrected to match the experimental and calculated maximum of the strong π– π* absorption at *ca.* 220 nm (the scaling factors are ranging from 1.08 for **1a** to 1.10 for **2b**). This procedure still left the calculated CD curves 10 nm blue-shifted. This is mainly due to an apparent blue shift of the experimental UV$_{max}$ position on the slope of the strong short-wavelength background absorption (Figure B, Supplementary Information). Otherwise, the calculated CD spectra of the parent cyclohexenone *cis*-diol **1a** and metabolites **1b–1d** were very similar to the experimental ones and also quite similar to each other, indicating only a small effect of the alkyl substituents at C3. This confirmed the absolute configuration of **1a** and **1b** as 4*R*,5*S*, as it was previously established by
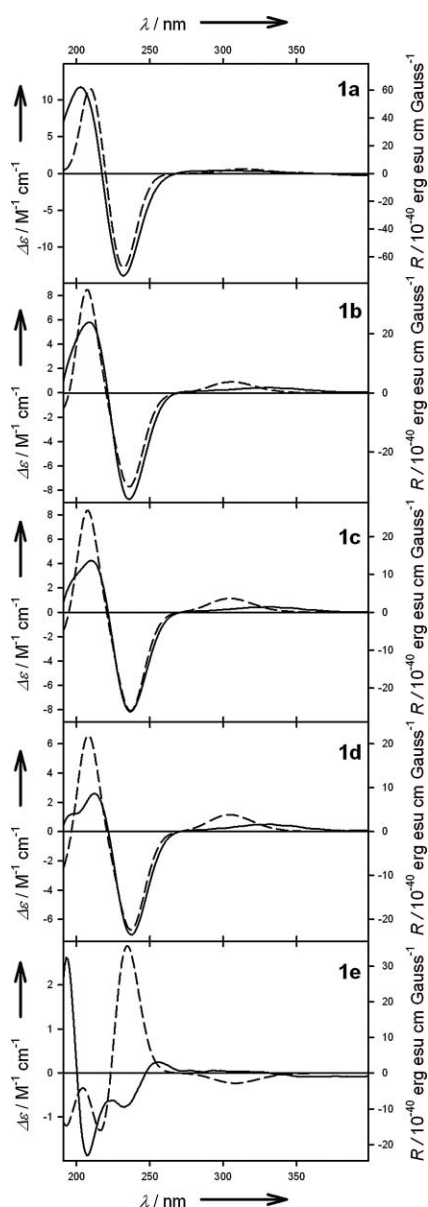
Fig. 3 CD spectra of *cis*-ketodiols **1a–1e**, experimental (in acetonitrile solutions, solid lines) and ΔE_{MP2} Boltzmann averaged calculated at PCM/B2LYP/Aug-cc-pVTZ level (dashed lines). Rotatory strengths R were calculated in dipole-velocity representation. All calculated spectra were wavelength-corrected to match the experimental short-wavelength UV λ_{max} at *ca.* 220 nm.

X-ray determination and chemical transformation of the 3-iodo derivative **1** (X = I)[7] into enone **1a** and established the absolute configuration of **1c** and **1d**.

The case of 3-*tert*-butyl substituted 2-cyclohexenone-*cis*-diol **1e** is apparently more complex, since the experimental CD spectrum is not reproduced well by computation for either enantiomer (Fig. 3). As is usually the case, the discrepancy between the experiment and the computation of chiroptical properties results from the incorrect computational reproduction of conformer population. The calculations show a low population (11%) of P conformers in the equilibrium with M conformers (89%) for molecules of **1e** *in vacuo* and even less (5–6%) in a polar
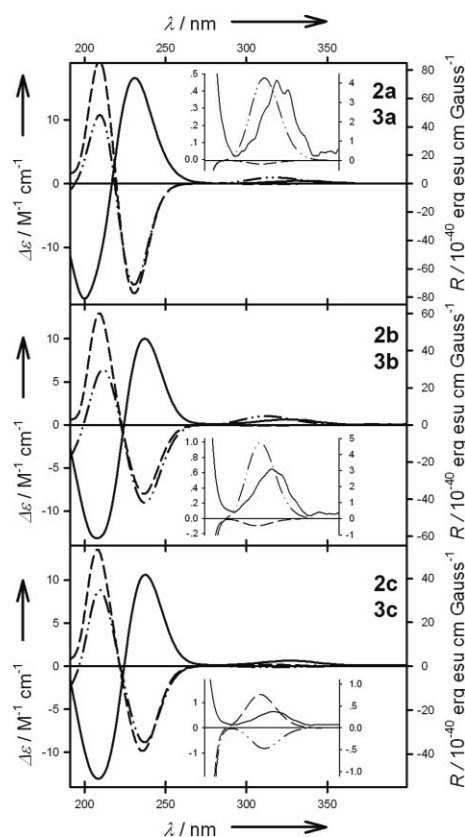
Fig. 4 CD spectra of *cis*-ketodiols *ent*-**2a–2c** experimental (in acetonitrile solutions, solid lines), ΔE_{MP2} Boltzmann averaged calculated at PCM/B2LYP/Aug-cc-pVTZ level for **2a–2c** (dashed lines) and **3a–3c** (dash-dot-dot lines). Rotatory strengths R were calculated in dipole-velocity representation. Inserts show $n_{C=O}$–$\pi_{C=O}^*$ transition region of the CD spectra. All calculated spectra were wavelength-corrected to match the experimental short-wavelength UV λ_{max} at *ca.* 220 nm.

environment. This is in sharp contrast to the results from structure calculations of the lower homologues **1a–1d** for which P-type conformers are the most abundant (up to 81% for **1a** in the acetonitrile continuous solvent model). In fact, a better agreement between the calculated and experimental CD curves was obtained if a higher ratio (> 70 : 30) of conformer $P4$ to $M4$ was assumed (these two conformers are the representative ones for acetonitrile solution), see Figure C, Supplementary Information. We noted that the method of geometry optimization has little effect on the further calculated ECD spectra.[¶] In the case of **1a**, **1b** and **1e** the geometries of individual conformers were re-optimized at the PCM/MP2/Aug-cc-pVTZ//PCM/MP2/6-311G(d,p) level of theory (see Tables B3 and B4 in Supplementary Information), followed by calculations of ECD spectra at the PCM/TDDFT/B2LYP/Aug-cc-pVTZ level of theory. Except for numerical values the results thus obtained were not different from those obtained with PCM/MP2/Aug-cc-pVTZ//PCM/B3LYP/6-311++G(2d,2p) method.

¶ During the work on the *cis*-ketodiols and other arene metabolites we tested various methods for calculation of molecular structure. These include different density functionals (with or without dispersion correction) and MO methods. Based on these results we did not observe any significant effect of long-range interactions on the conformation of molecules studied.

This journal is © The Royal Society of Chemistry 2010

Org. Biomol. Chem., 2010, **8**, 5635–5645 | 5639

Table 1 Specific optical rotations for *cis*-ketodiols **1–3**, measured in methanol solution and Boltzmann averaged calculated at the PCM/B3LYP/Aug-cc-pVTZ level (values in parentheses)

Diol	589 nm	578 nm	546 nm	436 nm
1a	−217 (−255)	−227 (−329)	−261 (−383)	−465 (−716)
1b	−119 (−103)	−124 (−140)	−141 (−162)	−237 (−287)
1c	−103 (−82)	−107 (−88)	−123 (−101)	−201 (−168)
1d	−79 (−72)	−82 (−62)	−94 (−71)	−150 (−112)
1e	−9 (+51)	−9 (+63)	−10 (+74)	−17 (+151)
2a	+223[a] (−264)	+234[a] (−340)	+273[a] (−399)	+540[a] (−814)
2b	+94[a] (−105)	+98[a] (−135)	+116[a] (−161)	+237[a] (−352)
2c	+104[a] (−96)	+109[a] (−144)	+128[a] (−168)	+259[a] (−377)
3a	(−239)	(−337)	(−387)	(−677)
3b	(−121)	(−185)	(−211)	(−343)
3c	(−108)	(−151)	(−171)	(−248)

[a] Measured for enantiomer.

The results of measurement and calculation of optical rotation for **1a–1d** are in agreement with the assignments obtained by ECD. Thus, the calculated and measured signs and magnitudes of specific optical rotations at four different wavelengths for **1a–1d** are in agreement with the assumed 4*R*,5*S* absolute configuration (Table 1, see also Table C in Supplementary Information). On the other hand, no such agreement is seen for *tert*-butyl substituted 2-cyclohexenone-*cis*-diol **1e**, for which the measured optical rotation is weakly negative, whereas the calculated rotations are positive. Since the calculated optical rotations of *P* conformers of **1e** are negative, the correct sign of optical rotation is obtained with over 50% population of these conformers in the equilibrium.

Thus, for **1e**, the discrepancy between the experimental and calculated OR data can be rationalised in the same manner as discussed above for the CD spectra of this compound.

For metabolites **2a–2c** having an additional alkyl substituent at C6, calculated and experimental CD spectra are of mirror-image type in the spectral region below 300 nm, indicating that the absolute configuration is reverse to that assumed, *i.e.* it is 4*S*,5*R*. This is indeed in agreement with the absolute configuration determined for the monocamphanate derivative of **2b**, using the X-ray diffraction method.[7]

Dihydroxyenones **3a–3c**, epimeric at C6, were used for computational assessment of CD spectra in order to differentiate between **2a–2c** and **3a–3c**. Unlike **2a–2c**, molecules of **3a–3c** are not restricted to conformers of *P* type (Fig. 2). Nevertheless, their CD spectra below 300 nm are deceptively similar to those of **2a–2c** (Fig. 4). The only difference between the calculated CD spectra of epimers **2a–2c** and **3a–3c** is the opposite sign of the *n*–π* Cotton effects at above 300 nm for each pair of epimers and slightly weaker positive Cotton effects at *ca.*: 210 nm for compounds **3a–3c**.

This computational study shows that the CD spectra of dihydroxyenones **1–3** reflect primarily the absolute configuration of these molecules at C4 and C5 and to a much lesser extent the conformation of the molecules. Namely, for 4*R*,5*S* absolute configuration a characteristic pattern of the Cotton effects is as follows: (+) *n*–π*, (−) π–π*, (+) third Cotton effect. Thus, the CD spectroscopy can be regarded as a reliable method for determining absolute configuration of 4,5-dihydroxy-2-cyclohexenones without resorting to computations. The only difficult cases are those having spherically unsymmetrical 3-alkyl (Et, *i*-Pr) substituents

on 2-cyclohexenones (**1c** and **1d**). In some of the calculated conformations the alkyl group attached to a sp² carbon atom generates a rotamer in which the methyl group is oriented perpendicularly to the C2═C3 bond (torsion angle φ 90–92°, conformers *M*1b, *M*2b, *M*3b, *M*4b of **1c** and φ 113–116° for the same conformers of **1d**, see Table B, Supplementary Information). Therefore the pseudoaxial methyl group of the substituent at the non-stereogenic C3 carbon atom contributes to the rotational strength of the *n*–π* and π–π* transitions in an opposite direction to that of the hydroxy substituent in C4 position, resulting in a change of the sign pattern of the dihydroxyenone Cotton effects.

A similar effect of conformation of the C3-alkyl substituent is seen in calculated optical rotations. In Fig. 5 is shown a selected example: ethyl-substituted keto-*cis*-diol **1c** (full version on Fig. 5 is deposited in Supplementary Information). Whereas OR values for the majority of conformers of **1a–1d** is negative (regardless whether *P* or *M* conformation), it is strongly positive for conformers mentioned above, *i.e.* *M*1b, *M*2b, *M*3b and *M*4b of **1c** and **1d**. Thus simple rotation of the ethyl or isopropyl group at the non-stereogenic carbon atom (C3) in **1c** or **1d** can dramatically change the chiroptical properties of the molecule.
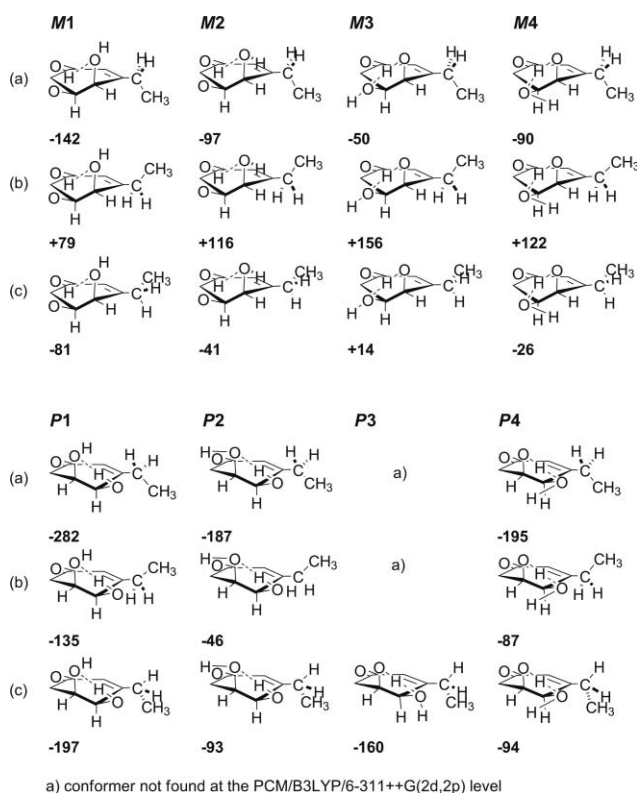
Fig. 5 Effect of rotation of hydroxy and ethyl substituents on the calculated (PCM/B3LYP/Aug-cc-pVTZ level) optical rotation at 589 nm for low-energy conformers of **1c**.

These findings clearly indicate that, in order to clarify the role of various constituents of a chiral enone structure in determining its chiroptical properties, calculations for simpler model compounds are necessary.

5640 | *Org. Biomol. Chem.*, 2010, **8**, 5635–5645

This journal is © The Royal Society of Chemistry 2010

3. Analysis of the calculated circular dichroism spectra of acrolein and model 2-cyclohexenones 4–23

3.1 Nature of the low-energy transitions

Acrolein (CH$_2$=CHCHO) is structurally the most simple model of an α,β-unsaturated carbonyl compound. The molecule can be chiral if it is nonplanar. Since the structures of acrolein and 2-cyclohexenone (**4**) differ significantly, the origin of calculated rotatory strengths may be different for both model compounds. We performed analysis of the electronic structures of acrolein and a number of 2-cyclohexenones by the natural bond orbital (NBO) method.[32] This method has a unique feature of analyzing the electron density by using sophisticated basis sets and methods in terms that are familiar to a chemist, such as Lewis structure, lone pairs, bonds, antibonds and Rydberg orbitals.

For planar acrolein the origin of the first two low-energy singlet transitions is clear: the long-wavelength electronic transition involves HOMO-1 and LUMO orbitals, whereas in the case of the next electronic transition the major contribution comes from the transition between HOMO and LUMO orbitals. The higher energy region is more complex, since there are three electronic transitions of similar energy at around 160 nm. These include HOMO-2–LUMO and HOMO-1–LUMO+2 transitions. According to the calculation the first electronic transition is $n_{C=O}$–$\pi_{C=O}^*$, the second $\pi_{C=C}$–$\pi_{C=O}^*$ and the third band is composed of $\pi_{C=O}$–$\pi_{C=O}^*$ and $n_{C=O}$–$\sigma_{C(O)-H}^*$ transitions (Fig. 6(a)).
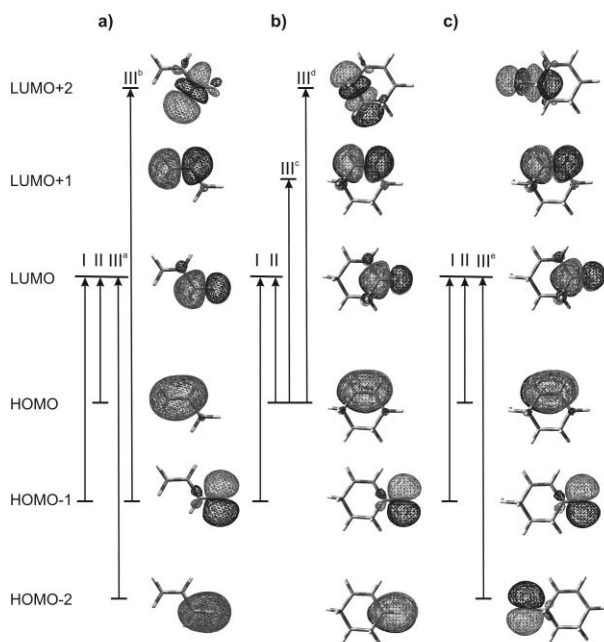
Fig. 6 Molecular orbitals obtained with the use of the NBO method for representative planar enones: acrolein (a) and *P*-type conformers of substituted 2-cyclohexenones **4** (b) and (4*S*)-**7** (c). I $n_{C=O}$–$\pi_{C=O}^*$, II $\pi_{C=C}$–$\pi_{C=O}^*$, III^a $\pi_{C=O}$–$\pi_{C=O}^*$, III^b $n_{C=O}$–$\sigma_{C(O)-H}^*$, III^c $\pi_{C=C}$–$\pi_{C=C}^*$, III^d $\pi_{C=C}$–$\sigma_{C-C}^*/\sigma_{C-H}^*$, IIIe n_{OH}–$\pi_{C=O}^*$.

In the case of 2-cyclohexenone (**4**) with either a planar or a twisted chromophore the first two electronic transitions, calculated at 286 nm and 211 nm, respectively, originate (in >80%) from the same orbitals as in the case of acrolein (see Fig. 6(b)). However,

a reverse order of the two transitions is suggested by calculations for 6-hydroxy substituted 2-cyclohexenones. The third electronic transition at *ca.* 180 nm is a mixture of $\pi_{C=C}$–$\pi_{C=C}^*$ transition (HOMO–LUMO+1, >80% contribution), $\pi_{C=C}$–σ_{C-C}^* and $\pi_{C=C}$–σ_{C-H}^* transitions (HOMO–LUMO+2, minor contributions) of low oscillator strength. This is a new finding on the origin of the short-wavelength transition and it is apparently in line with the previously postulated[16] sensitivity of the short wavelength transition in 2-cyclohexenone derivatives to the pattern of the C–C bonds in the vicinity of the enone C=C bond.

It should be noted that for the majority of methyl-substituted model compounds **5–23** (with a planar chromophore) the same order of interacting orbitals for the first two electronic transitions is retained, as is the case for 2-cyclohexenone (**4**). The third electronic transition in the case of 4,5-dimethyl derivatives **18** involves additionally HOMO-2 and LUMO orbitals ($\pi_{C=O}$–$\pi_{C=O}^*$ transition). However, in the cases of all hydroxy substituted 2-cyclohexenones the origin of the third electronic transition of low intensity, appearing at *ca.* 190 nm, is quite different and it involves the lone pair of the hydroxy group (HOMO-2) and LUMO orbitals, see Fig. 6(c), therefore constituting (typically in *ca.* 80%) the n_{OH}–$\pi_{C=O}^*$ transition. This new finding suggests that in the cases of hydroxylated 2-cyclohexenone derivatives the sign of the short wavelength electronic transition Cotton effect may be dependent on the helicity of the O–C–C=O bond system. Indeed, for epimeric 4-hydroxy-2-cyclohexenones (4*S*)-**7** and (4*R*)-**7** (a known phenol metabolite)[7] strong, opposite sign short-wavelength Cotton effects are calculated (see Figure D, Supplementary Information).

3.2 Contribution due to non-planarity of the enone chromophore

As it was mentioned earlier, a non-planar enone is an inherently dissymmetric (helical) chromophore. In addition, planar *s-trans* enones (torsion angle $\omega = 180°$) may be chiral due to non-planarity of the C=C bond or chiral disposition of the rest of the molecule. This is the case of 2-cyclohexenone (**4**), where at least one of the carbon atoms of the C4–C5–C6 bridge is out of the plane generated by the planar enone chromophore ($\omega = 180°$, $\tau = 0°$).

A good model for the enone chromophore can be acrolein. The molecule can be made helical by changing torsion angles ω and τ (the latter defined in this case as (O)C–C=C–H angle, where H is *syn* to (O)C–C bond) to form (+/+ or −/−) or (± or −/+) structures. For calculations the torsion angles ω and τ were varied in the range ±5°, in one degree steps. For all conformers the rotatory strengths were calculated at PCM/B2LYP/6-311++G(2d,2p) level. The results are shown in diagrams representing the calculated rotatory strengths for the first three electronic transitions as the functions of torsion angles ω and τ (see Figure E in Supplementary Information). Fig. 7 shows the cases where either the enone or the C=C bond is planar.

As expected, for a planar C=C bond, the calculated rotatory strengths support the enone helicity rule, for both $n_{C=O}$–$\pi_{C=O}^*$ and $\pi_{C=C}$–$\pi_{C=O}^*$ electronic transitions – a positive ω angle results in a negative $n_{C=O}$–$\pi_{C=O}^*$ and a positive $\pi_{C=C}$–$\pi_{C=O}^*$ rotatory strength. The short-wavelength electronic transition generates rotatory strength of opposite sign to the sign of the rotatory strength of the $\pi_{C=C}$–$\pi_{C=O}^*$ transition. It should be noted that unlike $n_{C=O}$–$\pi_{C=O}^*$ and $\pi_{C=C}$–$\pi_{C=O}^*$ transitions, the calculated
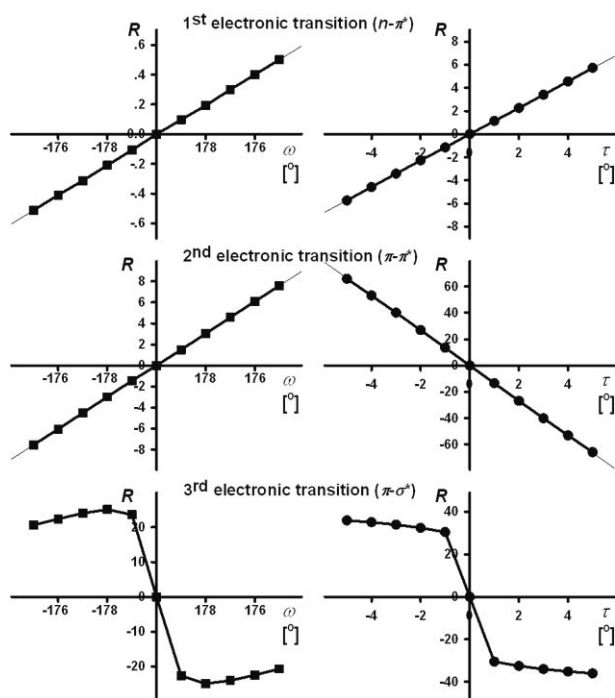
Fig. 7 Rotatory strengths R of the three low-energy electronic transitions of acrolein as a function of torsion angles ω and τ, calculated at PCM/B2LYP/6-311++G(2d,2p) level (left panels $\tau = 0°$, right panels $\omega = 180°$).

rotatory strength of the third electronic transition is not a simple function of angle ω.

On the other hand, for $\omega = 180°$, even a small deviation from planarity of the C=C bond generates rotatory strengths of the $n_{C=O}–\pi_{C=O}*$ and $\pi_{C=C}–\pi_{C=O}*$ transitions of much higher intensity (up to 10 times) compared to those calculated for a twisted acrolein model with a planar C=C bond. The sign dependence of the rotatory strengths of the $n_{C=O}–\pi_{C=O}*$ and $\pi_{C=C}–\pi_{C=O}*$ transitions on the sign of angle τ is opposite to that of angle ω, *i.e.* for a positive angle the τ calculated rotatory strengths are positive for the $n_{C=O}–\pi_{C=O}*$ and negative for the $\pi_{C=C}–\pi_{C=O}*$ transitions. Thus, one can conclude that the contribution to the calculated rotatory strength due to non-planarity of the C=C bond can override the contribution due to non-planarity of the enone chromophore. The acrolein model obeys the enone helicity rule when ω and τ angles are of opposite sign.

Similar analysis was performed for 2-cyclohexenone (**4**) (see Figure F in Supplementary Information). This case is more complex due to the presence of a non-planar saturated carbon chain by which the chromophore is embedded into the ring. An approximate contribution from that chain to the rotatory strength of a given electronic transition was obtained by subtraction of the rotatory strength calculated for acrolein from that obtained for conformers of 2-cyclohexenone **4** (see Figure G in Supplementary Information). The presence of the saturated carbon chain significantly affected the rotatory strengths of the $\pi_{C=C}–\pi_{C=O}*$ transition, especially for the structures where the enone was twisted "unnaturally" in *P*-type conformers, *i.e.* when ω was negative. Magnitudes, but not the signs, of the calculated rotatory strengths for the $n_{C=O}–\pi_{C=O}*$ transition were also affected by the presence of the C4–C5–C6 chain. The contribution of the C4–C5–C6 chain

Table 2 Averaged contributions of the rotatory strength ($R×10^{-40}$ erg esu cm Gauss^{-1}) to (*P*)-2-cyclohexenone (**4**) Cotton effects due to non-planarity of the enone chromophore

		$n_{C=O}–\pi_{C=O}*$	$\pi_{C=C}–\pi_{C=O}*$
$\omega = 175°$	$\tau = -2°$ to $2°$	-1.5	12
$\omega = -175°$	$\tau = -2°$ to $2°$	2	-8
$\tau = 2°$	$\omega = -175°$ to $175°$	2	-17
$\tau = -2°$	$\omega = -175°$ to $175°$	-2	17
$\tau = 5°$	$\omega = -175°$ to $175°$	9	-48
$\tau = -5°$	$\omega = -175°$ to $175°$	-7	55

was positive for all combinations of the enone and C=C twist angles in *P*-type conformers. For the reasons mentioned in the preceding section, analysis of the rotatory strength of the third electronic transition as a function of ω and τ torsion angles was not pursued.

The contribution of the C4–C5–C6 chain to the calculated rotatory strength of the $n_{C=O}–\pi_{C=O}*$ and $\pi_{C=C}–\pi_{C=O}*$ transitions in (*P*)-2-cyclohexenone with a planar enone chromophore is estimated correspondingly as $4.3 × 10^{-40}$ and $-5.6 × 10^{-40}$ cgs units.

The effect of non-planarity of the enone chromophore in 2-cyclohexenone **4** and its monosubstituted derivatives **5–11** could be assessed by subtracting the rotatory strength calculated for a molecule with a planar chromophore ($\omega = 180°$, $\tau = 0°$) from that of a molecule for which either ω or τ is varied within $\pm5°$ range (Table D, Supplementary Information). As in the case of acrolein, changes of either ω or τ resulted in significant changes of the rotatory strengths, shown in Table 2.

Comparable distortions of the C=C bond (angle τ) and enone chromophore (angle ω) resulted in a more significant rotatory strength change in the former case, the signs following the pattern determined for acrolein. The low-energy conformers of 2-cyclohexenone **4** with a twisted enone chromophore have torsion angles ω and τ of opposite sign (Table E, Supplementary Information), hence the contributions to the rotatory strengths due to non-planarity of the chromophore are partially cancelling.

A similar effect can be observed for 3-methyl-2-cyclohexenone **5** and (4*S*)-4-hydroxycyclohex-2-enone **7** (Figures H and I, Supplementary Information). In the latter case the rotational strengths of the low energy transitions are strongly dependent on angle τ, however due to the presence of the 4-hydroxy substituent, the signs of the rotatory strengths for $\pi_{C=C}–\pi_{C=O}*$ and $n_{OH}–\pi_{C=O}*$ transitions remain unchanged (correspondingly negative and positive).

3.3 Contributions due to the substituents

The investigated *cis*-diols **1–3** contain polar as well as alkyl groups around their cyclohexenone skeleton that may modify the CD spectra significantly. To determine the effect of the substituents we replaced systematically the hydrogen atoms at C3–C6 in 2-cyclohexenone **4** with either a polar hydroxy group or a non-polar methyl group (molecules **5–23**). The conformation of the hydroxy group was arbitrarily fixed antiperiplanar to the C*–H bond (see Figure J and Table D in Supplementary Information), except for molecules having an equatorial OH group at C6 where the H–O/C–H torsion angle was fixed at $-108°$. The structures of all molecules were fixed to have a planar chromophore. To estimate the effect of the substituent, the calculated rotatory strengths of these model compounds were divided by those

5642 | *Org. Biomol. Chem.*, 2010, **8**, 5635–5645

This journal is © The Royal Society of Chemistry 2010

calculated for a planar unsubstituted 2-cyclohexenone (Table F, Supplementary Information). Alternatively, the substituent effect could be determined by subtracting the calculated rotatory strength for a given transition of **4** from that of substituted 2-cyclohexenone.

Among monosubstituted 2-cyclohexenones **6–11**, substitution with either a methyl or a hydroxy group provides a negative (or very small positive) contribution to the rotatory strength of the $n_{C=O}$–$\pi_{C=O}^*$ transition, regardless of the position of the substituent. The most significant effects are noted for the hydroxy groups in 4-axial, 5-equatorial and 6-equatorial positions and for the methyl substituent in a 5-axial position.

As expected for the $\pi_{C=C}$–$\pi_{C=O}^*$ transition, the most significant changes to the calculated rotatory strengths are due to the substituents in the C4 (allylic) position. The effects due to the equatorial and axial substituents are of opposite sign. An equatorial substituent gives a strong negative contribution, in contrast to a positive contribution of the axial substituent in the *P* conformers, in effect revealing the helicity of the R–C$_{allyl}$–C=C system as negative for the equatorial and positive for the axial substituent. The effect of the allylic axial substituent appears insensitive to its polarity. In contrast, replacing an equatorial methyl by a hydroxy group (as in the cases of (4*S*)-**6** and (4*S*)-**7**), increases twofold the calculated rotatory strength of the 2-cyclohexenone derivative. This is apparently due to a better overlap of the polar C–O bond by HOMO, especially when the OH group is in the allylic equatorial position.

Substituents at C5 affect the CD spectrum strongly if they occupy an axial position. However, the contributions calculated for the methyl group (in (5*S*)-**8** and (5*R*)-**8**) and the hydroxy group (in (5*S*)-**9** and (5*R*)-**9**), are in pairs of opposite sign, adding complexity to the general scheme. Going further to the C6 position, the calculated rotatory strength for the axially methyl-substituted molecule (6*S*)-**10** is higher than that calculated for the equatorial epimer (6*R*)-**10**, while an opposite relationship holds for the hydroxy-substituted 2-cyclohexenones (6*R*)-**11** and (6*S*)-**11**. In addition, contributions due to the axial and equatorial substituents are mutually of opposite sign.

Based on the calculated rotatory strengths for the $\pi_{C=C}$–$\pi_{C=O}^*$ transition of monosubstituted (*P*)-2-cyclohexenones **5–11**, the substituent contributions, including signs, follow the sequence: 4eq-OH (−), 4ax-OH (+), 4ax-Me (+) > 4eq-Me (−), 5ax-OH (−), 6eq-OH (+) > 5ax-Me (+), 6ax-Me (−) > 5eq-OH (+), 5eq-Me (−), 6eq-Me (+), 6ax-OH (+). The dominant role of substituent at C4 over substituents either in C5 or C6 positions is clearly visible, regardless of their electronic nature and orientation (see Table F, Supplementary Information).

Specific optical rotations were calculated at the same level of theory for several monosubstituted 2-cyclohexenones **6–10** and for which experimental data are available in the literature (see Table G, Supplementary Information). Except for 2-cyclohexenone **10**, optical rotations at 589 nm, both calculated and experimental, are negative. This is apparently due to the substituent effect shown above *i.e.* negative contributions due to 4eq-Me, 4eq-OH, 5eq-Me or 5ax-OH, positive due to 6eq-Me.

In summary, going back to molecules **1** and **2**, and taking into account that their most dominant conformers are of *P*-helicity with the hydroxy groups occupying 4-equatorial and 5-axial positions, we can now order the structural factors contributing

most significantly to the rotatory strength of the $\pi_{C=C}$–$\pi_{C=O}^*$ transition. The contributions from non-planarity of the C=C bond and from the helicity of the HO–C–C=C system are of the same order of magnitude and much stronger than that due to non-planarity of the enone chromophore. The contribution due to an axial hydroxy group at C5 is also significant. A further possibility is that a better overlap of the equatorial oxygen at C4 by HOMO results in a higher value of the $\pi_{C=C}$–$\pi_{C=O}^*$ transition rotatory strength, compared to the methyl-substituted analogue. Thus, our study shows for the first time that the sign of the principal $\pi_{C=C}$–$\pi_{C=O}^*$ transition Cotton effect is less dependent on the enone non-planarity (angle ω) while being more dependent on the non-planarity of the C=C bond and the presence of a substituted helical 2-cyclohexenone ring. By way of example we compare the rotatory strengths of the $n_{C=O}$–$\pi_{C=O}^*$ and $\pi_{C=C}$–$\pi_{C=O}^*$ transitions, calculated either as a sum of contributions of structure elements or calculated directly for conformer *P*1 of dihydroxyenone **2a**. This conformer is representative as it contributes 70% to conformational equilibrium. The contributions to the rotatory strengths of the two lowest-energy transitions are correspondingly +5, −11 (2-cyclohexenone ring, $\omega = 175°$, $\tau = 1.6°$), 0, −68 (4eq OH group), −3, −33 (5ax OH group), −1, +9 (6eq Me group), data taken from Tables A, B and D, Supplementary Information). The sum of contributions, +1, −103 compares well with the data for this conformer +0.3, −113. Note that the relatively weak contribution of a helical *P* type 2-cyclohexenone ring is due to the cancelling effect of the twist of the enone and the C=C bond.
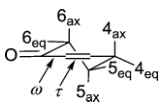
4. Conclusions

We have shown that the absolute configurations of 2-cyclohexenone *cis*-diols **1** and **2**, bacterial metabolites of phenols, can be determined by comparison of their experimental and calculated ECD spectra and optical rotations, despite the highly flexible nature of the molecules. By proper choice of the TDDFT method (PCM/B2LYP/Aug-cc-pVTZ), excellent agreement was obtained for most of the cases, despite the significant number of conformers and structural variables involved in the analysis (ring torsion angles, rotamers of the hydroxy and alkyl groups). It is shown that both the ECD spectra and optical rotations (including the sign) are also significantly affected by rotation of the ethyl or isopropyl substituent at C3.

The validity of the earlier postulated semiempirical helicity rules has been examined by calculations of the ECD spectra of a series of model enones using the above mentioned DFT method. Calculations confirmed that the two lowest-energy transition Cotton effects are predominantly of the $n_{C=O}$–$\pi_{C=O}^*$ and $\pi_{C=C}$–$\pi_{C=O}^*$ type and that their rotatory strengths are indeed dependent on the non-planarity of the enone chromophore (angle ω), as it was previously formulated within the *trans*-enone helicity rule. However, the present study shows that chiroptical behavior of 2-cyclohexenones is far more complex. The cyclohexenone ring is of C_1 symmetry and it contributes to the rotatory strengths according to its helicity (*P* or *M*). The C=C bond (angle τ) is not planar in low-energy conformers of substituted 2-cyclohexenones and this is a source of substantial contribution to the rotational strength of the two lowest-energy electronic transitions.

For the majority of low-energy conformers this contribution is of opposite sign to that due to non-planarity of the enone group.

Table 3 Signs of contributions to the rotatory strengths of the $n_{C=O}$–$\pi_{C=O}^*$ and $\pi_{C=C}$–$\pi_{C=O}^*$ Cotton effects of (P)-2-cyclohexenones
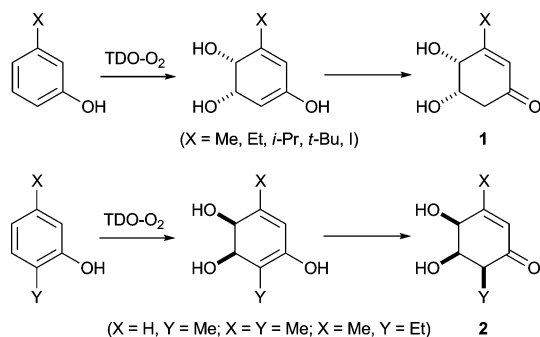

Contribution	$n_{C=O}$–$\pi_{C=O}^*$	$\pi_{C=C}$–$\pi_{C=O}^*$
P-helicity ring	+	—
(−)-ω	weak +	—
(−)-τ	—	+ to ++
4ax Me	—	+ +
4ax OH	—	+ +
4eq Me	ca. 0	– –
4eq OH	ca. 0	– –
5ax Me	—	+
5ax OH	—	– –
5eq Me	—	—
5eq OH	—	+
6ax Me	ca. 0	—
6ax OH	ca. 0	ca. 0
6eq Me	—	+
6eq OH	—	+ +

Furthermore, strong contributions to the rotatory strength of the $\pi_{C=C}$–$\pi_{C=O}^*$ transition are associated with a substituent (OH, Me) in positions 4 and 5. This is summarized in Table 3.

Another striking result of our study is the determination of the nature of the third band in the ECD spectra of 2-cyclohexenones. Calculations show that its nature is dependent on the presence of substituents. In 2-cyclohexenone and its alkyl derivatives it is predominantly a mixture of $\pi_{C=C}$–$\pi_{C=C}^*$ and $\pi_{C=C}$–σ^* transitions, whereas substitution with hydroxy groups results in a dominant contribution due to the n_{OH}–$\pi_{C=O}^*$ transition. Thus, although Cotton effects associated with these transitions may provide useful stereochemical information, their interpretation in any particular case will require computational analysis of the electronic transitions involved.

The single absolute configuration of enantiopure *cis*-dihydrodiol metabolites consistently obtained from TDO-catalysed *cis*-dihydroxylation of monosubstituted,[9] and *ortho*- or *meta*-disubstituted benzene substrates,[12] can now be rationalised on the basis of a simple model.[9,12] This contrasts with the enantiocomplementarity observed when enantiopure cyclohexenone *cis*-diols 1a–1e or 2a–2c of opposite configuration were formed using TDO and the corresponding phenols (Scheme 3). Further studies are in progress to identify more members of this new cyclohexenone *cis*-diol family and to use CD spectroscopy to establish (i) if opposite absolute configurations are consistently found for metabolite types 1 and 2 and (ii) if a predictive model for TDO-catalysed *cis*-dihydroxylation of phenols can also be developed.

Notes and references

1 B. L. Goodwin, in *Handbook of Biotransformations of Aromatic Compounds*, CRS, Press, Boca Raton, 2005.
2 D. R. Boyd, N. D. Sharma, J. S. Harrison, J. F. Malone, W. C. McRoberts, J. T. G Hamilton and D. B. Harper, *Org. Biomol. Chem.*, 2008, **6**, 1251.
3 R. A. Johnson, *Org. React.*, 2004, **63**, 117.
4 D. R. Boyd and T. D. H. Bugg, *Org. Biomol. Chem.*, 2006, **4**, 181.
5 K. A. B. Austin, M. Matveenko, T. A. Reekie and M. G. Banwell, *Chem. Aust.*, 2008, **75**, 3.
6 T. Hudlicky and J. W. Reed, *Synlett*, 2009, 685.
7 D. R. Boyd, N. D. Sharma, J. F. Malone and C. C. R. Allen, *Chem. Commun.*, 2009, 3633.
8 D. R. Boyd, N. D. Sharma, P. Stevenson, C. C. R Allen, L. Kulakov, H. Mundi, W. C. McRoberts and J. T. G. Hamilton, manuscript in preparation.
9 J. K. Gawronski, M. Kwit, D. R. Boyd, N. D. Sharma, J. F. Malone and A. Drake, *J. Am. Chem. Soc.*, 2005, **127**, 4308.
10 D. R. Boyd, N. D. Sharma, G. N. Coen, P. Gray, J. F. Malone and J. Gawronski, *Chem.–Eur. J.*, 2007, **13**, 5804.
11 M. Kwit, N. D. Sharma, D. R. Boyd and J. Gawronski, *Chem.–Eur. J.*, 2007, **13**, 5812.
12 M. Kwit, N. D. Sharma, D. R. Boyd and J. Gawronski, *Chirality*, 2008, **20**, 609.
13 M. Kwit, J. Gawronski, D. R. Boyd, N. D. Sharma, M. Kaik, R. A. More O'Ferrall and J. S. Kudavalli, *Chem.–Eur. J.*, 2008, **14**, 11500.
14 M. Kwit, J. Gawronski, L. Sbircea, N. D. Sharma, M. Kaik and D. R. Boyd, *Chirality*, 2009, **21**, E37.
15 R. D. Burnett and D. N. Kirk, *J. Chem. Soc., Perkin Trans. 1*, 1981, 1460.
16 J. K. Gawronski, *Tetrahedron*, 1982, **38**, 3.
17 N. Kirk, *Tetrahedron*, 1986, **42**, 777.
18 J. Gawronski, Conformations, Chiroptical and Related Spectral Properties of Enones, Chapter 3 in *The Chemistry of Enones*, S. Patai, Z. Rappoport, ed., J. Wiley, 1989.
19 D. A. Lightner and J. E. Gurst, *Organic Conformational Analysis and Stereochemistry from Circular Dichroism Spectroscopy*, Wiley-VCH, 2000.
20 G. Snatzke, *Angew. Chem., Int. Ed. Engl.*, 1979, **18**, 363.
21 G. Snatzke, in *Fundamental Aspects and Recent Developments in Optical Rotatory Dispersion and Circular Dichroism*, F. Ciardelli, P. Salvadori, ed., Heyden, London, 1973, pp. 109–124.
22 (a) G. Snatzke, *Tetrahedron*, 1965, **21**, 413; (b) G. Snatzke, *Tetrahedron*, 1965, **21**, 421.
23 C. Djerassi, R. Records, E. Bunnenberg, K. Mislow and A. Moscowitz, *J. Am. Chem. Soc.*, 1962, **84**, 870.
24 W. B. Whalley, *Chem. Ind.*, 1962, 1024.
25 W. Hug and G. Wagniere, *Helv. Chim. Acta*, 1971, **54**, 633.
26 (a) T. Liljefors and N. L. Allinger,, *J. Am. Chem. Soc.*, 1976, **98**, 2745; (b) J. K. Gawronski, T. Liljefors and B. Nordén, *J. Am. Chem. Soc.*, 1979, **101**, 5515.
27 G. Snatzke, *Tetrahedron*, 1965, **21**, 439; G. Snatzke, in *Optical Rotatory Dispersion and Circular Dichroism in Organic Chemistry*, G. Snatzke, Ed. Sadtler Research Labs, Inc, Philadelphia, 1967, pp. 208–223.
28 (a) H.-G. Kuball, S. Neubrech and A. Schönhofer, *Chem. Phys.*, 1992, **163**, 115; (b) H.-G. Kuball, B. Schultheis, M. Klasen, J. Frelek and A. Schönhofer, *Tetrahedron: Asymmetry*, 1993, **4**, 517; (c) J. Frelek, W. J.

(X = Me, Et, *i*-Pr, *t*-Bu, I)   **1**

(X = H, Y = Me; X = Y = Me; X = Me, Y = Et)   **2**

Scheme 3

5644 | *Org. Biomol. Chem.*, 2010, **8**, 5635–5645

This journal is © The Royal Society of Chemistry 2010

Szczepek, H. P. Weiss, G. J. Reiss, W. Frank, J. Brechtel, B. Schultheis and H.-G. Kuball, *J. Am. Chem. Soc.*, 1998, **120**, 7010; (*d*) J. Frelek, W. J. Szczepek, S. Neubrech, B. Schultheis, J. Brechtel and H.-G. Kuball, *Chem.–Eur. J.*, 2002, **8**, 1899.

29 A. W. Burgstahler and R. C. Barkhurst, *J. Am. Chem. Soc.*, 1970, **92**, 7601.

30 A. Diedrich and S. Grimme, *J. Phys. Chem. A*, 2003, **107**, 2524.

31 (*a*) N. Harada and P. Stephens, *Chirality*, 2010, **22**, 229; (*b*) N. M. O'Boyle, A. L. Tenderholt and K. M. Langner, *J. Comput. Chem.*, 2008, **29**, 839.

32 (*a*) F. Weinhold, in, *Encyclopedia of Computational Chemistry*, P. v. R. Schleyer, N. L. Allinger, T. Clark, J. Gasteiger, P. A. Kollman, H. F. Schaefer III and P. R. Schreiner, ed., John Wiley & Sons, Chichester, UK, 1998, Vol. 3, pp. 1792–1811; (*b*) A. E. Reed, L. A. Curtiss and F. Weinhold, *Chem. Rev.*, 1988, **88**, 899; (*c*) F. Weinhold and J. E. Carpenter, in, *The Structure of Small Molecules and Ions*, R. Naaman and Z. Vager, ed., Plenum, New York, 1988, pp. 227–236; (*d*) F. Weinhold, *Computational Methods in Organic Photochemistry: Molecular and Supramolecular Photochemistry*, A. G. Kutateladze, Ed., Taylor & Francis/CRC Press, Boca Raton FL, 2005, pp. 393–476.

This journal is © The Royal Society of Chemistry 2010

Org. Biomol. Chem., 2010, **8**, 5635–5645 | 5645